**Thickness dependent effects of an intermediate molecular blocking layer on the optoelectronic characteristics of organic bilayer photovoltaic cells.**

A. Steindamm[a,b], M. Brendel[a,b], A. K. Topczak[a] and J. Pflaum[a,b]

[a]Julius-Maximillians University, Am Hubland, 97074 Würzburg, Germany

[b]ZAE Bayern, Am Hubland, 97074 Würzburg, Germany

Abstract:

In this work we address the microscopic effects related to the implementation of a Bathophenanthroline (BPhen) exciton blocking layer (EBL) sandwiched between Ag cathode and molecular Diindenoperylene (DIP)/$C_{60}$ bilayer of a photovoltaic cell. Complementary studies of current density, external quantum efficiency, and photoluminescence quenching for EBL thicknesses up to 50 nm indicate that Ag atoms are able to penetrate through the whole 35 nm thick $C_{60}$ film into the crystalline DIP layer underneath, thereby enhancing exciton quenching if no blocking layer is applied. In contrast, an optimal trade-off between exciton blocking, suppression of metal penetration and electron transport is achieved for a 5 nm thick BPhen layer yielding an improvement of power conversion efficiency by more than a factor of 2.

Organic photovoltaic cells (OPVCs) have received considerable attention due to their potential for low cost, large-area preparation on flexible substrates and their individual opto-electronic properties associated with the chemical variety of their molecular constituents. Furthermore, the high absorption coefficients of molecular materials enable devices comprising photoactive layers of at most 100 nm thickness to absorb a substantial amount of the incident light. Hence interface properties become more and more crucial for the overall performance of OPVCs.

In this regard, non-radiative decay of excitons at organic/metal interfaces has been identified as a prominent loss channel in thin film OPVCs. To suppress this mechanism an additional exciton blocking layer (EBL) is implemented between the photoactive organic layers and the contact featuring a high bandgap to prevent optical excitations from reaching the metal interface.[1] Ideally the EBL supports efficient charge extraction by its high electron mobility and its matching with the relevant transport level of the acceptor. Peumans and Forrest demonstrated that for standard CuPc/$C_{60}$ bilayer cells a Bathocuproine (BCP) EBL yields an increase of the efficiency by a factor of 2.[2] However, the intuitive expectation that monolayer thick EBLs might be sufficient to prevent close proximity of excitons to metal interfaces and thereby non-radiative decay has proven deficient as many studies reported on superior OPVC performances for EBL thicknesses between 5 and 7 nm.[3,4] These observations indicate that not only preventing excitons from reaching the contact interface has to be considered by applying an EBL but also the formation of a penetration barrier for metal atoms upon contact deposition. Especially for crystalline films the latter is of fundamental importance as radio-tracer measurements revealed large penetration depths of metal atoms into molecular thin films[5] which considerably increase the probability of OPVC failure by short-circuiting.

Coping with these substantially different functionalities an optimum EBL thickness has to be identified at which protection of excitons from quenching as well as suppression of metal penetration together with a sufficiently good charge transport across the EBL are achieved. To aim for this goal and to develop a microscopic picture of processes related to the EBL we present a complementary approach by analyzing the characteristics of thin film photovoltaic devices as a

function of EBL thickness in combination with optical photoluminescence studies. Our OPVC model system consists of Bathophenanthroline (BPhen) as EBL in a prototypical Diindenoperylene/$C_{60}$ bilayer heterostructure. DIP has proven to be a suited donor material in combination with the acceptor $C_{60}$ resulting in planar heterojunction cells with open circuit voltages up to 0.9 V, exceptionally high fill factors of 74% and overall cell efficiencies of 4%.[6] Though the highest occupied molecular orbital (HOMO) and lowest unoccupied molecular orbital (LUMO) of BPhen are comparable to those of BCP, we focus on the former as its electron mobility has shown to be at least as high as for BCP and, in view of technical application, the long term stability of BPhen exceeds that of BCP.[7,8] Furthermore, in combination with Ag cathodes a better performance of BPhen EBLs compared to BCP was observed.[9]

OPVCs were prepared on PEDOT:PSS (Clevios$^{TM}$ P AI4083) covered ITO substrates. Thermal evaporation of the organic and metal layers has been carried out at base pressures of $10^{-8}$ mbar with substrates kept at room temperature. To avoid degradation photoelectric measurements of the external quantum efficiency (EQE) and the $j(V)$ characteristics were performed *in-situ* after device preparation without breaking the vacuum. According to preliminary studies on the optimum thicknesses of the photoactive layers we chose 30 nm of Diindenoperylene as donor and 35 nm of $C_{60}$ (CreaPhys) as acceptor, both materials were gradient sublimated twice. Bathophenanthroline (Sigma-Aldrich) EBLs of various thicknesses were deposited on one half of the DIP/$C_{60}$ stack while the other half was used as reference. Finally, 60 nm thick Ag cathodes of 2 mm circular diameter were thermally deposited through a shadow mask.

Samples for PL measurements consist of DIP (30 nm) and $C_{60}$ (35 nm) consecutively deposited on a glass substrate. To enable identical film conditions, one half of the $C_{60}$ on top was directly covered with 60 nm Ag, while the other half comprised a step-like intermediate BPhen EBL with thicknesses between 5 nm and 50 nm. As confirmed by supplementary X-ray analysis, the DIP layers are single crystalline across the entire film thickness whereas $C_{60}$ as well as BPhen layers turned out to be X-ray amorphous. For each BPhen thickness the PL generated at 532 nm excitation wavelength was measured on a BPhen covered area and was normalized to the

intensity of the corresponding area without EBL. By this procedure temporal fluctuations of the laser intensity were compensated. Comparative AFM studies on the OPVCs revealed similar surface roughness between 2 nm to 4 nm for the Ag top-layer with and without underlying BPhen EBL. Therefore morphological effects of the DIP/$C_{60}$ stack on the observed sample behavior were considered to be negligible.

Fig. 1 shows the *in-situ* measured $j(V)$-curve of a DIP(30nm)/$C_{60}$(35nm) bilayer cell without and with 5 nm BPhen layer between $C_{60}$ acceptor and Ag cathode. As can be seen the short circuit current density ($jsc$) of the bilayer OPVC with BPhen layer is almost doubled whereas the open circuit voltage and fill-factor change only slightly. Overall the $j_{sc}$ enhancement leads to an improvement of the device efficiency from 1.1% to 2.4% despite the barrier for electron transport expected by the LUMO level position of the intermediate BPhen layer (inset Fig. 1).

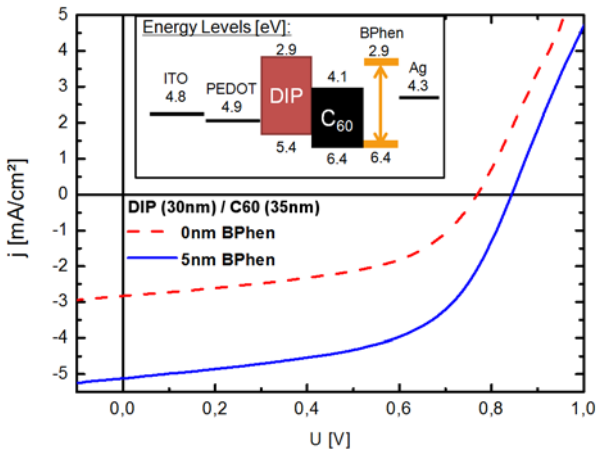


Fig. 1: *j(V)* curves of a DIP (30 nm)/$C_{60}$(35 nm) cell without (dashed line) and with an intermediate 5 nm BPhen EBL (solid line). The inset shows the energy levels of the used materials according to ref.[10,11,12], neglecting possible interface dipoles at the BPhen EBL.

To investigate the impact of the EBL on the power conversion efficiency as well as on the charge carrier transport we systematically varied the BPhen thickness and analyzed the corresponding OPVC characteristics. Since BPhen, according to its optical gap of about 3.5 eV, acts as a transparent optical spacer in the visible, the incident light is reflected at the Ag back electrode and

modulates the absorption profile in the DIP/$C_{60}$ bilayer cell due to interference effects. Therefore, the photocurrent data has to be normalized for the integral absorption which was determined by directional UV-VIS measurements in the relevant wavelength range between 300 nm and 700 nm for each BPhen thickness. Overall, the interference correction reveals deviations of less than 15% with respect to the pristine values presumably due to the interface topology of the individual layers within the molecular stack and therefore does not significantly affect the qualitative thickness dependence of the photophysical properties. As one of the most sensitive parameters, the absorption corrected short-circuit current density as a function of the BPhen layer thickness is displayed in Fig. 2 a).

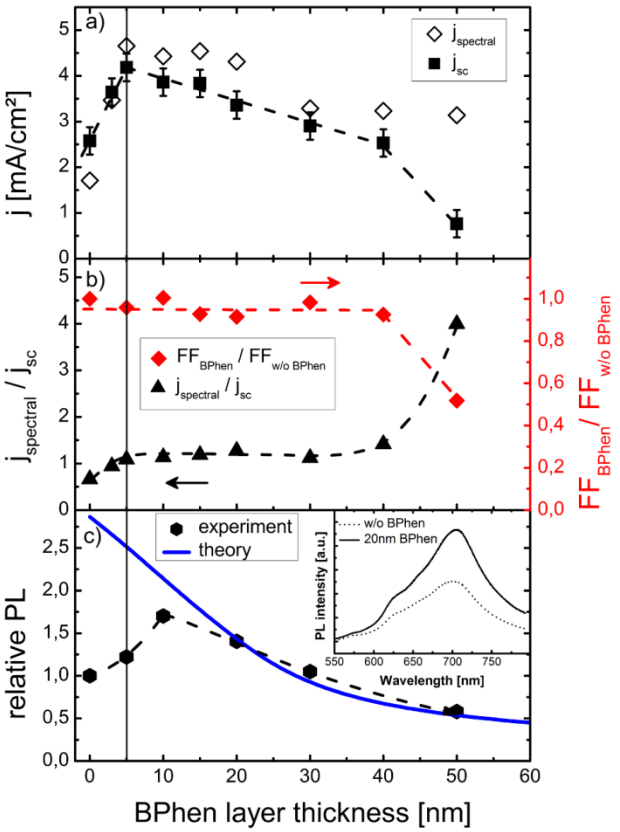


Fig. 2: Characteristics of DIP(30nm)/$C_{60}$(35nm)/BPhen(X)/Ag OPVCs as a function of BPhen thickness: a) densities of the absorption normalized short-circuit current $j_{sc}$ and spectral photocurrent $j_{spectral}$, and b) ratio between $j_{sc}$ and $j_{spectral}$ as well as fill factor *FF* normalized to a reference cell without BPhen on each substrate. Obviously, the photocurrents show a distinct maximum at a BPhen layer thickness of 5 nm. c) Normalized photoluminescence (PL) intensity

together with a theoretical model (solid line) considering interference effects, exciton diffusion and quenching. The inset shows the spectrally resolved PL of two representative samples. Dashed lines represent guides to the eye.

A pronounced almost linear increase of $j_{sc}$ (black squares) can be observed for thin BPhen films reaching its maximum at about 5 nm. This increase of short-circuit current density for thin BPhen layers can be attributed to the protection of excitons from reaching the Ag cathode interface, thereby minimizing non-radiative quenching due to the increasing EBL coverage. Suppression of Ag penetration into the exciton transport regions by the intermediate BPhen layer diminishes exciton quenching further. As a result, the total amount of excitons contributing to the photocurrent by dissociation at the DIP/$C_{60}$ interface is significantly enhanced. The dark currents at -0.5 V reverse-bias (not shown) accounted for less than 1% of the corresponding $j_{sc}$ at 1 sun (AM 1.5) for all devices evidencing that diminishing of shunts by inserting BPhen is not the main reason for the increased currents. Above 5 nm BPhen layer thickness $j_{sc}$ drops with an accelerated decrease for thicknesses above 40 nm. This general tendency can be qualitatively explained by the unfavorable position of the BPhen LUMO (3.2 eV) with respect to the electron transport level of $C_{60}$ (4.1 eV) both are listed in the inset of Fig. 1. Nevertheless, the fact that even for several tens of BPhen monolayers the photocurrent is still of comparable size than without EBL raises questions on the underlying transport mechanism and its relation to the film morphology.

To gain detailed access on this subject we have performed measurements on the external quantum efficiency (EQE) of the devices discussed in Fig. 2 a). As can be seen by Fig. 3 the $C_{60}$ contribution to the spectral photocurrent at about 450 nm drastically increases for BPhen thicknesses between 5 nm and 15 nm. Comparison with the absorption spectra (inset Fig. 3) highlights that the main contribution to the $j_{sc}$ enhancement emanates from the $C_{60}$ layer. Moreover, the EQE signals for EBLs thinner than 30 nm confirm the suppression of non-radiative exciton quenching to be the main reason for the photocurrent increase in this thickness regime in agreement with Fig. 2 a). In contrast, for cells with thicker EBL a disproportionate reduction of $C_{60}$

photocurrent at 450 nm versus that of DIP at 510 nm can be detected. This effect points to a reduced electron transport across the EBL for larger thicknesses, primarily affecting the photocurrent contributed by the $C_{60}$ acceptor layer.

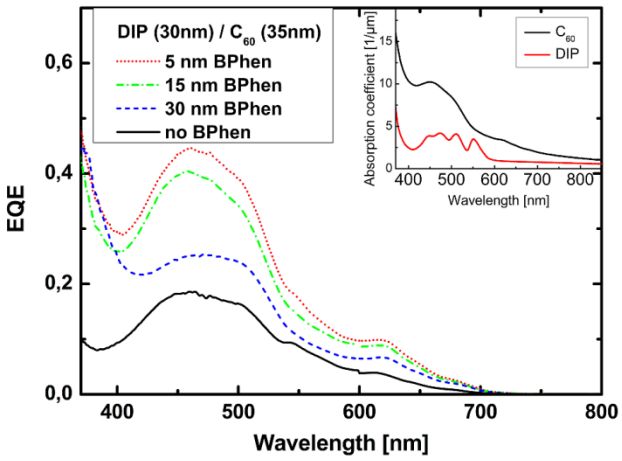


Fig. 3: External quantum efficiencies (EQE) of DIP(30nm)/$C_{60}$(35nm)/BPhen(X) bilayer cells with EBL thicknesses of 0 to 30 nm. The inset shows the absorption coefficient of $C_{60}$ and DIP single layers, respectively.

To conclude on the influence of metal induced trapping states on charge carrier transport in the devices we compared the integrated spectral photocurrent ($j_{spectral}$) and $j_{sc}$. The former can be calculated from the EQE by

$$j_{spectral} = \int \frac{EQE(\lambda) \cdot P_{AM1.5}(\lambda) \cdot q \cdot \lambda}{h \cdot c} \, d\lambda$$

where $P_{AM1.5}$ is the reference solar spectral irradiance and, $q$ and $\lambda$ are the elementary charge and the wavelength, respectively and is plotted, absorption normalized like $j_{sc}$, in Fig. 2 a). It is important to notice, that EQE measurements were performed without bias light and that the integrated light intensity equals to about 10 mW/cm² (~ 0.1 sun), i.e. $j_{spectral}$ represents the case of low light intensities normalized to theoretical current densities at 1 sun (AM1.5). This allows for

evaluation of material inherent effects on the charge carrier transport without significant influence by e.g. space-charging. Therefore, the ratio $j_{spectral}\ /j_{sc}$ shown in Fig. 2b) provides an indicator for the transport phenomena occurring in the DIP/$C_{60}$ bilayer cells.

While for BPhen layer thicknesses between 5 nm and 30 nm $j_{spectral}\ /j_{sc}$ roughly amounts to 1 this behavior significantly changes for samples without EBL ($j_{spectral}\ /j_{sc} \approx 0.7$). A smaller ratio indicates higher current losses for lower light intensities which can be explained by an enhanced trap density in the device, in particular at the $C_{60}$/Ag or $C_{60}$/BPhen/Ag interface, when no or only 3 nm EBL are present. By their continuous filling at higher light intensities these traps play a less dominant role for $j_{sc}$ at 1 sun (AM 1.5) than for the spectrally resolved photocurrent. As a possible origin for such trap states we identified the penetration of metal atoms into the photoactive $C_{60}$ layer during contact deposition.[5] Accompanied by cluster formation this leads to pronounced non-radiative exciton quenching in the acceptor layer in agreement with smaller photocurrents observed in EQE and under white light illumination.

Penetration of Ag into the EBL can also explain the observed electron transport behavior for thicker BPhen layers. As suggested by Chan et al.[11] for BPhen as well as by Rand and co-workers for BCP[13], metal induced trap states might be generated due to penetration which support transport of electrons even across thicker EBLs, coinciding with the ohmic-like $j_{sc}$ behavior for BPhen thicknesses between 5 and 40 nm in Fig. 2a). Finally, for BPhen layers above 40 nm thickness we observe a strong increase of $j_{spectral}\ /j_{sc}$ to about 4, indicating that for this thickness range charge transport at high illumination intensities is substantially limited, presumably by space charging at the $C_{60}$/BPhen interface, if silver atoms are not longer able to diffuse across the whole BPhen layer.[14,15] This coincides with the observed decrease in the fill factor (FF) of devices with BPhen thickness above 40 nm (Fig. 2b).

These results raise the question whether the current increase upon insertion of a BPhen EBL is caused by effects at the $C_{60}$/BPhen/Ag interface or by additional contributions descending from regions located even deeper inside the device and induced by Ag penetration into the photoactive molecular semiconductors. To investigate the extent of metal penetration spectrally resolved

photoluminescence (PL) measurements have been conducted on similar DIP(30nm)/$C_{60}$(35nm) bilayer structures deposited on glass substrates, subsequently covered by BPhen layers of different thickness and 60 nm Ag top-contacts. Since for $C_{60}$ relaxation from the lowest $S_1$ singlet state to the ground state is dipole forbidden and in addition is reduced by intersystem crossing to the triplet state[16], no spurious PL intensity arises from the acceptor layer. Therefore, effects on the DIP excitons caused by the blocking layer or by metal penetration can be directly identified by this technique.

The representative PL spectra for a DIP/$C_{60}$ bilayer sample with 20 nm BPhen EBL (solid line) and without BPhen (dashed line) are shown in the inset of Fig. 2 c). The shape of the spectra is almost identical but a strong PL enhancement for the sample with intermediate BPhen layer is evident. For a thickness dependent comparison the integrated spectral PL intensity of DIP/$C_{60}$ samples with BPhen/Ag coverage is normalized to the corresponding PL intensity without EBL and plotted in Fig. 2 c). A steep increase of the relative PL signal to a maximum of 1.7 at 10 nm BPhen thickness is observed, followed by a monotonous decrease for samples with thicker EBL leading to a relative PL of 0.6 for the 50 nm thick BPhen layer. The occurrence of the $j_{sc}$ maximum at 5 nm BPhen thickness compared to the peak of the relative PL at 10 nm (Fig. 2) is ascribed to a slightly different surface corrugation of the DIP layer on the glass substrate used for PL measurements and to space-charge induced current limitations in OPVCs with thicker EBL[14] that might already reduce the currents at 10 nm BPhen thickness. As for the currents, a quantitative interpretation of the data requires consideration of interference effects by the optical BPhen spacer. However, since both $C_{60}$ and DIP absorb light at the excitation wavelength of 532 nm but only DIP excitons contribute to the PL signal, correction by UV-VIS data cannot be applied in this case. Therefore, the exciton generation profile in the DIP layer has been calculated by the transfer matrix method for each sample architecture. The steady state exciton profile was then determined by an exciton diffusion model[17] implying boundary conditions of zero-quenching at the glass contact and complete dissociation at the interface with $C_{60}$. As a remark, though we assumed in our calculations an exciton diffusion length of 100 nm as reported in literature[18] any diffusion length exceeding the DIP thickness of 30 nm renders similar results. The theoretical PL, which is defined by the integrated

exciton concentration, was fitted to the relative PL intensity measured for the various BPhen thicknesses (solid line in Fig. 2 c). As can be seen by the figure, for EBL thicknesses above 10 nm the theoretical curve reproduces the experimental PL behavior quite well. However, for thinner BPhen layers the measured PL decreases significantly and yields to a pronounced deviation from the theoretical predictions.

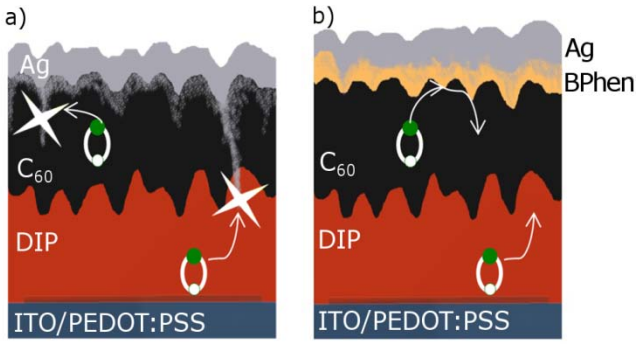


Fig. 4: a) Schematic picture of exciton quenching processes due to metal penetration into the photoactive organic layers. b) By the intermediate BPhen EBL (yellow layer) metal penetration and therefore non-radiative exciton losses become effectively suppressed.

This behavior can be rationalized by Ag penetration even through the 35 nm thick $C_{60}$ layer if no or only an incomplete EBL is present, leading to metal accumulation and thus enhanced exciton quenching at the DIP interface or along DIP grain boundaries as sketched in Fig. 4. This microscopic picture is in good agreement with the previously discussed photocurrent measurements, which suggested an increased trap density in the photoactive molecular materials for BPhen layer thickness below 5 nm.

In summary we demonstrated a doubling of the short-circuit current in DIP/$C_{60}$ bilayer photovoltaic cells by implementation of a 5 nm BPhen EBL, raising the total device efficiency to 2.4%. From thickness dependent analyses of the photocurrent we conclude that electron transport across the EBL preferentially takes place by metal induced trap states, whose concentration is significantly reduced for BPhen thicknesses above 40 nm. Complementary photoluminescence studies on the

DIP donor layer revealed the current increase upon EBL insertion to be ascribed to both, blocking of excitons directly at the Ag cathode interface and prevention of metal penetration into the photoactive molecular film stack. Thereby, the combination of photocurrent and PL quenching measurements has proven to be a powerful approach to identify excitonic processes in the distinct regions of layered OPVCs.

Acknowledgements:

The authors thank S. Höhla and S. Hirschmann (University of Stuttgart) for the preparation of ITO substrates and for material purification. A. Wagenpfahl (University of Würzburg) is acknowledged for providing the optical simulation software. This work was supported by the BMBF-Project GREKOS and the DFG-Project SPP1355.

[1]P. Peumans, V. Bulovic, and S. R. Forrest, Appl. Phys. Lett. **76**, 2650 (2000).

[2]P. Peumans, and S. R. Forrest, Appl. Phys. Lett. **79**, 126 (2001).

[3]Z. R. Hong, Z. H. Huang, and X. T. Zeng, Thin Solid Films. **515**, 3019 (2007).

[4]S. M. B. Ghorashi, A. Behjat, and R. Ajeian, Sol. Energ. Mat. Sol. C. **96**, 50 (2012).

[5]M. Scharnberg, J. Hu, J. Kanzow, K. Rätzke, R. Adelung, F. Faupel, C. Pannemann, U. Hilleringmann, S. Meyer, and J. Pflaum, Appl Phys Lett. **86**, 024104 (2005).

[6]A. Opitz, J. Wagner, W. Brütting, I. Salzmann, N. Koch, J. Manara, J. Pflaum, A. Hinderhofer, and F. Schreiber, IEEE J. Sel. Top. Quant. **16**, 1707 (2010).

[7]M. Ichikawa, J. Amagai, Y. Horiba, T. Koyama, and Y. Taniguchi, J. Appl. Phys. **94**, 7796 (2003).

[8]S. Naka, H. Okada, H. Onnagawa, and T. Tsutsui, Appl. Phys. Lett. **76**, 197 (2000).

[9]N. Wang, J. Yu, H. Lin, and Y. Jiang, Chin. J. Chem. Phys. **23**, 84 (2010).

[10]J. Wagner, M. Gruber, A. Hinderhofer, A. Wilke, B. Bröker, J. Frisch, P. Amsalem, A. Vollmer, A. Opitz, N. Koch, F. Schreiber, and W. Brütting, Adv. Funct. Mater. **20**, 4295 (2010).

[11]M. Y. Chan, C. S. Lee, S. L. Lai, M. K. Fung, F. L. Wong, H. Y. Sun, K. M. Lau, and S. T. Lee, J. Appl. Phys. **100**, 094506 (2006).

[12]M. Chelvayohan, and C. H. B. Mee, J. Phys. C: Solid State Phys. **15**, 2305 (1982).

[13]B. P. Rand, J. Li, J. Xue, R. J. Holmes, M. E. Thompson, and S. R. Forrest, Adv. Mater. **17**, 2714 (2005).

[14]S. Wang, T. Sakurai, R. Kuroda, and K. Akimoto, Appl. Phys. Lett. **100**, 243301 (2012).

[15]The measured EBL range has been extended to even thicker BPhen layers of 100 nm. However, the reliability and significance of this data is strongly limited by the small currents and therefore has been omitted in this discussion.

[16]J. W. Arbogast, A. P. Darmanyan, C. S. Foote, Y. Rubin, F. N. Diederich, M. M. Alvarez, S. J. Anz, and R. L. Whetten, J. Phys. Chem. **95**, 11 (1991).

[17]P. Peumans, A. Yakimov, and S. R. Forrest, J. Appl. Phys. **93**, 3693 (2003).

[18]D. Kurrle, and J. Pflaum, Appl. Phys. Lett. **92**, 133306 (2008).